Contrast Variation in Light Scattering: Silica Spheres Dispersed in Apolar Solvent Mixtures

A. K. VAN HELDEN AND A. VRIJ

Van't Hoff Laboratory for Physical and Colloid Chemistry, Transitorium 3, Padualaan 8, 3584 CH Utrecht, The Netherlands

Received September 10, 1979; accepted November 1, 1979

The contrast variation method, well known from small-angle neutron and X-ray experiments, is applied to a light-scattering study of colloidal dispersions of spherical particles. The theory is rederived in terms of light-scattering parameters and extended to cases of preferential adsorption of one of the solvent components at the particle surface. Experiments were carried out with spherical monodisperse lyophilic silica dispersions in (binary) mixtures of cyclohexane and *trans*-decaline. It is found that the silica particles have a low mean refractive index and that significant optical density variations occur in the particle. Cyclohexane is preferentially adsorbed. For the system under consideration the light-scattering contrast variation method appears to be a valuable technique for particle characterization.

I. INTRODUCTION

Contrast variation is at present a well-known method in small-angle X-ray and neutron scattering of biological macromolecules and colloidal particles [see, e.g., Stuhrmann *et al.* (1, 2), White *et al.* (3), and Taupin *et al.* (4)]. It is essentially based on a continuous variation of the scattering contrast of the solvent in which the particles are embedded which is accomplished by a variation of the composition of a mixture of two (or more) solvents with different scattering length. The method comprises the determination of parameters like particle size and mean scattering length, as well as spatial distribution of scattering length inside the particle.

The principle of the method is not unknown in light scattering. It was applied earlier, e.g., to determine the molar mass of polyelectrolytes and micelles in electrolyte solutions by changing the scattering power of the coion (5, 6). It is also used now to characterize polymer molecules with two or more different scattering elements [block copolymers, e.g. (7)]. In this paper we will present the results of a contrast variation study that is more akin to the small-angle X-ray and neutron scattering case, i.e., a continuous variation of the solvent refractive index in a dispersion of *compact* colloidal particles.

The theory of contrast variation for X-ray and neutron scattering has been treated in detail (1, 8). The principles are directly transferable to light scattering when the contrast is sufficiently small [the so-called Rayleigh–Gans–Debye (RGD) regime]. The theory is complex and involves an expression of the spatial distribution of scattering dipoles inside the particles in terms of orthogonal polynomials.

In the next section we will rederive some important equations in terms of light-scattering parameters, in which a somewhat different, more elementary route will be followed which is sufficiently general when the angular variation of the scattering intensity is weak, as is often the case in light scattering. We will further extend the theory to cases where there is a preferential adsorp-

0021-9797/80/080418-16$02.00/0

tion of one of the solvent components at the particle surface. This effect is probably unimportant in neutron scattering where the solvent mixtures contain different elemental isotopes which are "chemically" practically identical. In light scattering, however, the contrast can be changed only by using (mixtures of) chemically different molecules which may have different interactions with the particle surface. The theory will be applied to light scattering measurements on silica spheres, dispersed in mixtures of cyclohexane and *trans*-decaline.

These phenomena are of particular importance when studying concentrated dispersions by the light-scattering method. Generally this will be impossible for particles with a size larger than say 10 nm because of the large optical densities which give rise to multiple scattering effects. In such cases it is essential to reduce the excess scattering power of the particles drastically by choosing the refractive index of the medium near to that of the particles (9, 10).

II. THEORY

The light-scattering theory for discrete, homogeneous particles in the Rayleigh–Gans–Debye (RGD) approximation is well known (11). For dilute systems the normalized, excess scattering intensity of a dispersion over that of the solvent medium per unit volume (Rayleigh ratio) is proportional to the particle number density ρ,

$$R(K) = \rho\sigma(K), \qquad [1]$$

where $\sigma(K)$ is the "scattering cross section" of one particle which for vertically polarized incident light is given by,

$$\sigma(K) = \mathcal{H}^*(n_p - n_0)^2V^2P(K), \qquad [2]$$

with,

$$\mathcal{H}^* = 2\pi^2n^2\lambda_0^{-4}. \qquad [3]$$

Here n_p, n_0, and n are the refractive indices of particle, solvent, and dispersion respectively and V is the particle volume. Further $P(K)$ is an intraparticle interference factor depending on $K = (4\pi n/\lambda_0) \sin(\theta/2)$, where θ is the scattering angle and λ_0 the wavelength of the light *in vacuo*. For small K,

$$P(K) = 1 - R_g^2K^2/3 + \cdots, \qquad [4]$$

where R_g is the radius of gyration of the particle. In the RGD approximation: $n_p - n_0 \ll n_0$.

To describe the scattering of an optically nonhomogeneous particle, consider the particle as built up by a set, $\{\omega\}$, of volume elements dV_ω with refractive index n_ω. The volume elements have an equal size $dV_\omega = dV$, their number being $N = V/dV$. Then the quantity $(n_p - n_0)V$ in Eq. (2)—here called the scattering amplitude Q—must be replaced by the sum,

$$Q = \sum_\omega q_\omega \equiv (\bar{n}_p - n_0)V, \qquad [5]$$

where q_ω is the amplitude of element dV_ω, given by,

$$q_\omega = (n_\omega - n_0)dV. \qquad [6]$$

Equation [5] also defines the mean refractive index of the particle, $\bar{n}_p$. The "optical" radius of gyration is given by,

$$R_g^2 = Q^{-1} \sum_\omega q_\omega\rho_\omega^2, \qquad [7]$$

where $\rho_\omega = |\boldsymbol{\rho}_\omega|$ is the distance of element dV_ω from the optical center Z of the particle. The position of Z is defined by,

$$\sum_\omega q_\omega\boldsymbol{\rho}_\omega = 0. \qquad [8]$$

Then one obtains for $\sigma(K)$,

$$\sigma(K)/\mathcal{H}^* = Q^2\left[1 - \frac{K^2}{3}Q^{-1}\sum_\omega q_\omega\rho_\omega^2\right]. \qquad [9]$$

Now it is important to realize that this representation is *not* convenient when considering contrast variation, because the position of Z will depend on n_0 through the Eqs. [6] and [8]. In fact, Z moves out of the particle to infinity when $n_0 \to \bar{n}_p$!

To circumvent this difficulty another representation is clearly desirable. This can be found by an explicit formulation of each q_ω as an average plus a fluctuation on the average, thus:

$$q_\omega = \bar{q} + \Delta q_\omega,$$
$$\bar{q} = (\bar{n}_p - n_0)dV,$$
$$\Delta q_\omega = (n_\omega - \bar{n}_p)dV. \quad [10]$$

Note that $\sum_\omega \Delta q_\omega = 0$. Now it is natural to consider instead of the set of elements $\{\omega\}$ three subsets $\{\alpha\}$, $\{\beta\}$, and $\{\gamma\}$. In subset $\{\alpha\}$, containing the same elements as $\{\omega\}$, all volume elements have the same refractive index $\bar{n}_p$. Subset $\{\alpha\}$ represents what is called the "equivalent homogeneous particle." The subsets $\{\beta\}$ and $\{\gamma\}$ also run over the same elements as $\{\omega\}$ but the volume elements have refractive indices larger, respectively smaller than $\bar{n}_p$, i.e., $\Delta q_\beta > 0$ and $\Delta q_\gamma < 0$. This transforms Eq. (5) into,

$$Q = Q_\alpha + Q_\beta + Q_\gamma,$$
$$Q_\alpha = \sum_\alpha \bar{q} = \bar{q}N = (\bar{n}_p - n_0)V,$$
$$Q_\beta = \sum_\beta \Delta q_\beta; \quad Q_\gamma = \sum_\gamma \Delta q_\gamma,$$
$$Q_\beta + Q_\gamma = 0; \quad |Q_\beta| = |Q_\gamma|. \quad [11]$$

Now all three subsets have *fixed* optical centers because $\bar{q}$ is equal in all volume elements and Δq_β and Δq_γ are independent of n_0. Calling these centers A, B, and C, respectively, and vectors originating from them by $\boldsymbol{\rho}_\alpha$, $\boldsymbol{\rho}_\beta$, and $\boldsymbol{\rho}_\gamma$, the positions of these centers are defined by,

$$\sum_\alpha \bar{q}\boldsymbol{\rho}_\alpha = \bar{q} \sum_\alpha \boldsymbol{\rho}_\alpha = 0,$$
$$\sum_\beta \Delta q_\beta \boldsymbol{\rho}_\beta = 0; \quad \sum_\gamma \Delta q_\gamma \boldsymbol{\rho}_\gamma = 0. \quad [12]$$

Remember that the optical center Z of the (whole) *particle* was given by Eq. [8]. As a next step the position vectors with respect to Z are now expressed in position vectors with respect to A (see Fig. 1), thus,

$$\text{set } \{\alpha\}: \quad \boldsymbol{\rho}_\omega = \boldsymbol{\rho}_\alpha - \mathbf{r}_Z,$$
$$\text{set } \{\beta\}: \quad \boldsymbol{\rho}_\omega = \boldsymbol{\rho}_\beta + \mathbf{r}_B - \mathbf{r}_Z,$$
$$\text{set } \{\gamma\}: \quad \boldsymbol{\rho}_\omega = \boldsymbol{\rho}_\gamma + \mathbf{r}_C - \mathbf{r}_Z, \quad [13]$$

where $\mathbf{r}_Z$, $\mathbf{r}_B$, and $\mathbf{r}_C$ are the positions of Z, B, and C with respect to A. Using Eq. [8] one finds with Eqs. [10], [13], and [11] that,

$$Q\mathbf{r}_Z = Q_\beta(\mathbf{r}_B - \mathbf{r}_C) \equiv \boldsymbol{\mu}. \quad [14]$$

Note that $\boldsymbol{\mu} = Q_\beta(\mathbf{r}_B - \mathbf{r}_C)$ constitutes the "optical dipole moment" of the particle. Further, substitution of Eqs. [13] into Eq. [7] gives,

$$R_g^2 = Q^{-1}\{\bar{q} \sum_\alpha |\boldsymbol{\rho}_\alpha - \mathbf{r}_Z|^2 + \sum_\beta \Delta q_\beta |\boldsymbol{\rho}_\beta + \mathbf{r}_B - \mathbf{r}_Z|^2 + \sum_\gamma \Delta q_\gamma |\boldsymbol{\rho}_\gamma + \mathbf{r}_C - \mathbf{r}_Z|^2\}. \quad [15]$$

Then using Eqs. [12] and [13] one obtains after some simple algebra,

$$R_g^2 = R_{g0}^2 + Q^{-1}(T_\beta + T_\gamma) - Q^{-2}\mu^2 \quad [16]$$

and

$$\sigma(K)/\mathcal{K}^* = Q^2\left(1 - \frac{K^2R_{g0}^2}{3}\right) - \frac{K^2Q}{3}(T_\beta + T_\gamma) + \frac{K^2\mu^2}{3}. \quad [17]$$

Here R_{g0} is the radius of gyration of the equivalent homogeneous particle. The "optical moments of inertia" T_α, T_β, T_γ of the subsets $\{\alpha\}$, $\{\beta\}$, and $\{\gamma\}$ with respect to A, are given by,

$$T_\alpha = \bar{q} \sum_\alpha \rho_\alpha^2 = QR_{g\alpha}^2 \equiv QR_{g0}^2,$$
$$T_\beta = \sum_\beta \Delta q_\beta \rho_\beta^2 + Q_\beta r_B^2 = Q_\beta(R_{g\beta}^2 + r_B^2),$$
$$T_\gamma = \sum_\gamma \Delta q_\gamma \rho_\gamma^2 + Q_\gamma r_C^2 = Q_\gamma(R_{g\gamma}^2 + r_C^2), \quad [18]$$

where $R_{g\alpha}(=R_{g0})$, $R_{g\beta}$ and $R_{g\gamma}$ are the radii of gyration of the three subsets. Obviously,

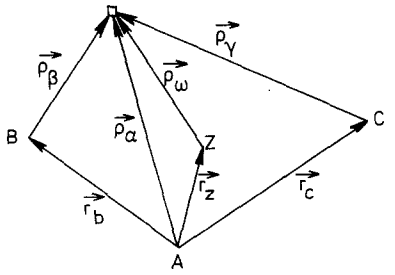

FIG. 1. Position vectors and optical centers of the total particle, the equivalent homogeneous particle, and the subsets, respectively. Further explanation is given in the text.

R_{g0}, T_β, T_γ, and μ are independent of n_0. On inspection of Eq. [16] it will be clear that the concept "radius of gyration" looses its physical meaning when $n_0 \to \bar{n}_p$ (and thus $Q \to 0$) because R_g^2 may become very large and even negative because T_β and T_γ are of opposite sign and the term containing μ^2 is always negative. The intensity, however, as given by Eq. [17] remains positive for $Q \to 0$ as it should.

Accessibility of Solvent; Preferent Adsorption

Up to now it was implicitly assumed that the accessibility of solvent to the particle (measured by V) is independent of the solvent or solvent mixture. This is a good approximation when the solvent is a mixture of isotopes as in neutron scattering. In light scattering, however, one has to use a mixture of different species. It cannot be assumed a priori that the accessibility of different solvent molecules to the particle (surface) will be identical. Also "surface forces" may be different and may preferentially attract one of the solvent species. The—from a practical point of view—ill-defined notion of V and also of n_p can be circumvented by invoking the fluctuation theory of light scattering (12). For pure solvents, simply make the substitution:

$$Q = (\bar{n}_p - n_0)V = (dn/dc_p)m, \quad [19]$$

where dn/dc_p and m, the particle mass, are both measurable quantities. Here c_p is the particle concentration in mass per volume. Equation [19] may then be considered as defining $\bar{n}_p$, with $V = m/\delta$ and δ the particle density (i.e., the reciprocal partial specific volume of the particle). It has indeed been found experimentally, as Eq. [19] implies, that dn/dc_p is a linear function of n_0 [for polymers in pure solvents (13)] which is necessary for the contrast variation method to apply. For mixed solvents the fluctuation theory of light scattering gives, see, e.g. (14), that dn/dc_p should be replaced by $(\partial n/\partial c_p)_{\mu_s}$, i.e., the refractive index increment should be measured (in an osmotic cell) at constant chemical potentials of the solvent components. One can write (14),

$$(\partial n/\partial c_p)_{\mu_s} = (\partial n/\partial c_p)_\psi + \Gamma(\partial n/\partial \psi)_{c_p} \quad [20]$$

$$\Gamma = (\partial \psi/\partial c_p)_{\mu_s} \quad [21]$$

where ψ is a measure of the composition of the solvent, e.g., the mole fraction of component 1, and Γ denotes the preferent adsorption of that component. For $c_p \to 0$, $(\partial n/\partial \psi)_{c_p} = dn_0/d\psi$.

The influence of preferent adsorption on the interpretation of the K^2 term in the scattering is more complex because this term depends on the spatial distribution of the preferently adsorbed species which, in general, may change with solvent contrast in an unknown, complicated fashion. We, therefore, have to impose certain limitations on the further analysis to keep it tractable and will restrict to a particle having a compact structure with a thin surface layer, preferential adsorption taking place only in this layer. Then, in addition to the amplitudes defined in Eq. [10], we introduce an excess (surface) amplitude,

$$q_\sigma = (n_\sigma - n_0)dV_\sigma$$

$$Q_\sigma = \sum_\sigma q_\sigma. \quad [22]$$

Here $n_\sigma - n_0$ is the excess refractive index in a surface element dV_σ. Let us make this more explicit for our system: SiO_2-particles

with alkane chains terminally attached to the particle surface. If in a given single-component solvent the scattering amplitudes of the particle—attached chains included—are given by Eqs. [10], then the elements dV_σ are the layers of solvent near the particle surface and among the attached chains having a refractive index difference with the solvent far away from the particle of $n_\sigma - n_0$. In a given pure solvent $n_\sigma - n_0 = 0$ by definition, but in a solvent mixture n_σ may be a complicated function of n_0 and the local position on the particle surface. In another pure solvent, $n_\sigma - n_0$ may in principle be different from zero, due to differences in the local densities of the pure solvents near the surface. This effect, if perceptible, would show up as a deviation of the linear dependence on n_0 as given by Eq. [19]. In practice we identify Q_σ with the excess term in Eq. [21], i.e.,

$$Q = m(\partial n/\partial c_p)_\psi,$$

$$Q_\sigma = m\Gamma(\partial n/\partial \psi)_{c_p}. \quad [23]$$

To describe the influence of specific adsorption on the angular dependence we will restrict our analysis to the case that the position $\mathbf{r}_S$ (with respect to A) of the optical center S of the collection $\{\sigma\}$—the adsorbed layer—is independent of n_0. Incorporating this in the previous derivations it is found that instead of Eq. [14] one obtains,

$$(Q + Q_\sigma)\mathbf{r}_Z = Q_\beta(\mathbf{r}_B - \mathbf{r}_C) + Q_\sigma \mathbf{r}_S, \quad [24]$$

$$R_g^2 = R_{g0}^2 + (Q_\beta/Q_t)(R_{g\beta}^2 + r_B^2 - R_{g\gamma}^2 - r_C^2) + (Q_\sigma/Q_t)(R_{g\sigma}^2 + r_S^2 - R_{g0}^2) - (\boldsymbol{\mu} + Q_\sigma \mathbf{r}_S)^2 Q_t^{-2}, \quad [25]$$

and

$$\sigma(K)/\mathcal{K}^* = Q_t^2(1 - K^2R_g^2/3), \quad [26]$$

where $R_{g\sigma}$ is the radius of gyration of the excess scattering amplitude Q_σ (with respect to S) due to preferent adsorption, and $Q_t = Q + Q_\sigma = m(\partial n/\partial c_p)_{\mu_s}$. Finally one may introduce an excess refractive index of the particle, $\Delta\bar{n}_p$,

$$Q = (\bar{n}_p - n_0)V; \quad Q_\sigma = \Delta\bar{n}_p V. \quad [27]$$

When either Q_σ or $\Delta\bar{n}_p$ can be determined from the scattering intensity at $K = 0$, it can be used in Eq. [25] to assess the contribution of adsorption to R_g.

Polydispersity

For a polydisperse system Eq. [1] becomes,

$$R(K) = \sum_i \rho_i \sigma_i(K) = \rho\langle\sigma(K)\rangle, \quad [28]$$

where i runs over the different particles, $\rho = \sum_i \rho_i$ and $\langle\sigma\rangle \equiv (\sum \rho_i\sigma_i)/\rho$ is a (number) average of σ. Using, e.g., Eq. [17] one observes that this results in the quantities: $\langle Q^2\rangle$, $\langle Q^2R_{g0}^2\rangle$, $\langle Q(T_\beta + T_\gamma)\rangle$, and $\langle\mu^2\rangle$. The average squares are always positive, but $\langle Q(T_\beta + T_\gamma)\rangle$ may be positive or negative. Further one may observe that for a polydisperse system the contrast variation procedure, which is based on a linear relationship between $\langle Q^2\rangle^{1/2}$ and n_0, must break down when $\langle Q\rangle \to 0$: the value of $R(K = 0)$ will not become zero at any n_0 but attain a minimum value at $\langle Q\rangle = \langle(n_p - n_0)V\rangle = 0$. The magnitude of the minimum gives $\langle(Q - \langle Q\rangle)^2\rangle$ which thus depends on fluctuations both in size and refractive index of the particles, which are possibly correlated depending on the process of particle growth.

III. MATERIALS AND METHODS

The lyophilic silica (sample S7) was prepared in two steps. First a silica dispersion was prepared in ethanol (alcosol) by the method of Stöber *et al.* (15). Absolute ethanol (Merck) and ammonia (Merck) were mixed in different ratios and freshly distilled ethylorthosilicate (Fluka) was added. The mixture was stirred at ambient temperature; the reaction was completed in 2–5 hr. According to Stöber *et al.* the final particle size is determined by the initial concentration of water and ammonia. The concentrations of the reactants were (in mole dm^{-3}):

water, 2.5; ammonia, 0.95; ethylorthosilicate, 0.15.

The silica was rendered lyophilic by chemisorption of stearylalcohol at the surface of the particle. The method has been reported by Iler (16). The alcohol molecules are chemically linked with surface silanol groups by a condensation reaction. The reaction is completed at 180°C under nitrogen atmosphere. The product was purified from excess stearylalcohol by centrifuging the silica dispersions in cyclohexane and discarding the supernatant. The procedure was repeated three times. The silica was dried overnight. The dry powdery product thus obtained was readily dispersable in alifatic solvents.

The light-scattering measurements were performed with a Fica 50 light scattering photometer (Société Francaise d'Instruments de Controle et d'Analyse). As scattering standard pure benzene was used ($R_{90} = 15.8 \times 10^{-6}$ cm^{-1} at $\lambda_0 = 546$ nm and 45.6×10^{-6} cm^{-1} at $\lambda_0 = 436$ nm). The experiments were carried out with the 546 and 436 nm line (unpolarized) of a Philips CS 100 W/Z mercury arc lamp. The measurements were carried out at 25 ± 1°C.

Transmission electron microscope measurements were performed with a Philips EM 301 apparatus, provided with a Plumbicon television tube and image intensifier. Carrier grids covered with carbon-coated Parlodion films were dipped in a dilute dispersion and electron micrographs were taken of the particles retained on the film.

Light scattering fluctuation spectroscopy was performed with a laboratory built instrument containing a double walled thermostated sample holder (25.0 ± 0.1°C). The 514.5 nm line of an Ar-ion laser (Spectra Physics model 165) was used and the light was detected by an EMT 9558 photonmultiplier. The correlation function was determined with a Saicor-Honeywell 42A correlator, with photon counting option. The correlation functions were analyzed numerically.

IV. PARTICLE CHARACTERIZATION

Electron Microscopy

The silica dispersion was characterized by electron microscopy, to determine the shape, size, and size distribution of the particles. The particles are spherical to a good approximation (see Fig. 2). The size distribution is shown in Fig. 3. The number average radius $\langle a_{EM} \rangle_n$ was 53 nm with a standard deviation of 9.7%. Comparison of the electron microscopy result with the data obtained from light scattering fluctuation spectroscopy (given in Table I) shows that the former technique yields a smaller radius than the latter one. Accurate measurements, which were carried out with a similar sample, showed that the silica particles shrink as a result of radiation damage. The decrease in size was ~5% (17). If we use this number and correct the electron microscopy result for the radiation damage, a discrepancy still remains, which cannot be explained satisfactorily. A slight difference in size is expected, because the aliphatic chain molecules will be expanded in a good solvent, contrary to a more collapsed configuration in the dry phase. This, however, is compensated by the fact that the electron microscopy measures the number average radius, whereas light-scattering fluctuation spectroscopy yields a z-average diffusion coefficient (at high contrast), from which the radius is calculated; $\langle (1/a) \rangle_z$. Actually one should compare $\langle (1/a)_{EM} \rangle_z^{-1}$, calculated from the EM size distribution of Fig. 2, with the light-scattering fluctuation spectroscopy result. It was found that $\langle (1/a)_{EM} \rangle_z^{-1}$ was only 1 nm smaller than $\langle a_{EM} \rangle_n$.

Light-Scattering Fluctuation Spectroscopy

Light-scattering fluctuation spectroscopy measurements were performed to characterize the dispersion in the solvent phase. The autocorrelation function of the scattered intensity was determined at different scattering angles. The relaxation time τ_R

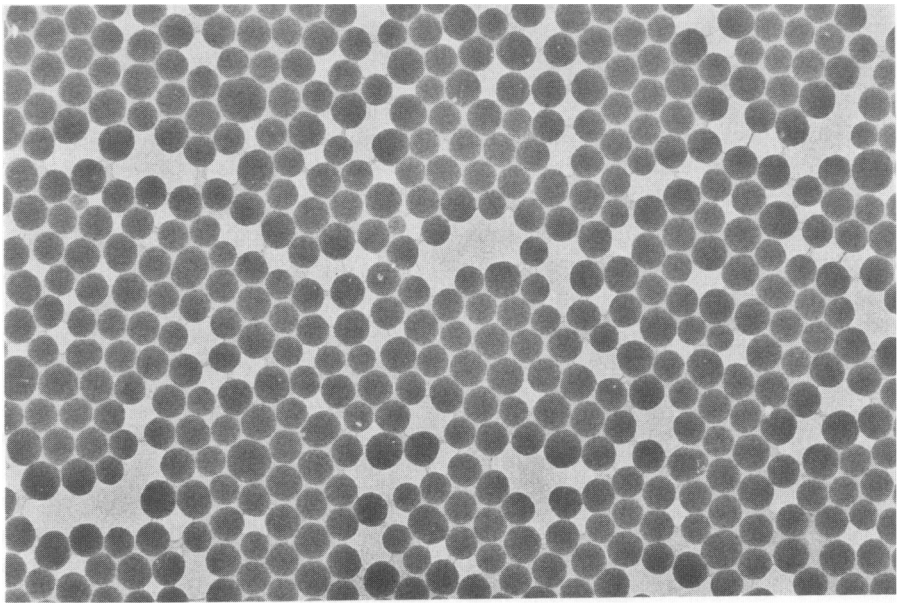

FIG. 2. Electron micrograph of the lyophilic silica particles (sample S7) as taken from a suspension in cyclohexane.

thus found is related to the diffusion coefficient D according to,

$$\tau_R^{-1} = 2DK^2. \quad [29]$$

From the diffusion coefficient the hydrodynamic radius a_D of the particles is calculated using the Stokes–Einstein relation,

$$D = kT(6\pi\eta a_D)^{-1}, \quad [30]$$

where η is the viscosity of the solvent. The silica dispersion was measured in binary mixtures of cyclohexane and *trans*-decaline with molefraction *trans*-decaline from 0 to 1. The experiments were carried out with dilute dispersions. The highest concentration was 2.9 g dm^{-3}. Equation [29] shows that the diffusion coefficient is determined from the slope in a plot of the reciprocal relaxation time versus the wave vector squared. The linear dependence, which is found for all systems at high values of K^2, indicates monodisperse particles and the slope is used to calculate the hydrodynamic radius, a_D. The sizes found in the different solvents (mixtures) are almost equal, regarding the experimental error in the diffusion coefficient measurement. The results are shown in Table I. Frequently a curvature was found, however, in the lower K^2-region. The decreasing slope points to the existence of "hydrodynamic units" with a lower diffusion coefficient. Probably this means that some clustering of particles occurs in the solution, since electron microscopy results showed that the size distribution of the primary particles is narrow. The presence of these clusters does not contribute significantly to the scattering at large angles, because the particle-scattering function falls off rapidly with increasing wave vector. We may summarize that the hydrodynamic size of the particles is approximately constant in different media. The interactions between the particles however change with varying chemical composition of the medium and may induce some cluster formation in several systems. As a result of the cluster formation the scattering data in the low K^2-region do not contain information about the primary particles and only the higher K^2-range ($>2 \times 10^{+14}$ m^{-2}; $\lambda_0 = 514$ nm) is appropriate to study the individual particles.

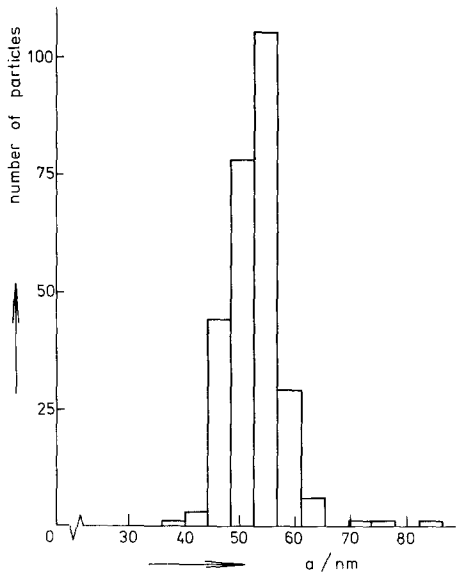

FIG. 3. The size distribution of the silica particles determined from electron microscopy. The number of particles is plotted as a function of radius a. The total number of counted particles is 269. The number average radius $\langle a_{EM} \rangle_n$ is 53 nm.

V. INTENSITY OF SCATTERED LIGHT

Contrast Variation

Measurements of the (time-averaged) light-scattering intensity were performed with the same sample. The dispersions were prepared by starting from a dilute dispersion in cyclohexane (2.9 g dm^{-3}) and adding subsequently different amounts of *trans*-decaline into the cuvet. The dilution factor was determined by weighing. It was less than 3.4. The scattered intensity was measured as a function of scattering angle and composition of the solvent medium. It was found that the scattering intensity, extrapolated to $K = 0$, as well as the angular dependence changes remarkably with the composition of the medium. Some results are shown in Fig. 4. Here the Rayleigh ratio is divided by the concentration c (w/v) to correct the scattering data for dilution. $R(K)/c$ is plotted on a logarithmic scale versus K^2. It may be noticed from Fig. 4 that (a) the scattering intensity extrapolated to zero angle depends on the composition of the medium and is minimal at intermediate compositions and maximal in the pure component media; (b) the angular dependence is linear at higher values of K^2 and the slope is a function of the composition of the medium; (c) for low scattering intensities a pronounced curvature in the angular dependence appears in the low K^2-region.

We believe that this curvature reflects the presence of small amounts of clustered particles, which become more apparent at low contrast. This explanation was also suggested by Cebula *et al.* (3), who measured polystyrene latices in H_2O-D_2O mixtures with neutron scattering. Also in the light-scattering fluctuation spectroscopy results the presence of clustered particles is more pronounced for solvent compositions with low contrast. We shall not use the intensity data at low K^2-values in the further interpretation, because extrapolation to $K \to 0$ is difficult. We will focus our attention now on the data of higher scattering angles, where the influence of clusters is optically not detectable anymore. Extrapolation of the scattering intensity to zero scattering angle is performed from the region with higher K^2.

By changing the composition of the medium one also changes the refractive index n_0. From the Eqs. [1], [9], and [5] we see that the scattering intensity is proportional to $(\bar{n}_p - n_0)^2$. The scattering dependence described in (a) is easily understood in view of this. A numerical evaluation enables the determination of the mean refractive index and the molar mass of the particle. Introducing the weight concentration c_p (g

TABLE I

Radius, a_D, of Silica Particles as Determined from Light-Scattering Fluctuation Spectroscopy in Mixtures of Cyclohexane and *t*-Decaline

Mole fraction of *t*-decaline	0.00	0.41	0.54	1.00
a_D (nm)	62.5	64.4	64.0	62.8

cm^{-3}) one finds from Eqs. [1] and [2] for $K \to 0$ and $c \to 0$,

$$n_0^{-1}[R(K = 0)(2c_p)^{-1}]^{1/2} = [\mathcal{K}'M]^{1/2}(\bar{n}_p - n_0), \quad [31]$$

where $\mathcal{K}' = 2\pi^2(\lambda_0^4 \mathcal{N}_{AV}\delta^2)^{-1}$ and δ is the mass density of the particles. The factor 2 in the left-hand side of Eq. [31] appears because of the $(1 + \cos^2\theta)$ term for unpolarized incident light. By plotting $n_0^{-1}[R(K = 0) \times (2c_p)^{-1}]^{1/2}$ versus n_0, a linear dependence must be found. The slope contains the square root of the molar mass $M = \mathcal{N}_{AV}m$. The intersection with the n_0-axis yields $\bar{n}_p$. Values for n_0 were taken from Johnson and Smith (18) for cyclohexane and *t*-decaline (λ_0 = 546 and 436 nm). The refractive index of intermediate compositions was calculated with the Lorentz–Lorenz equations (see Ref. 18) using experimentally determined densities (19). In Fig. 5 results are shown for particles in cyclohexane diluted with *t*-decaline. Except for very low intensities near the matching point, i.e., zero contrast, good linearity was found. Numerical values of the slope $[\mathcal{K}'M]^{1/2}$ and the intercept $\bar{n}_p$ are given in Table II. Departure from linearity near $n_0 = \bar{n}_p$ is expected because of polydispersity (see Section II); such points were discarded. Stuhrmann and Duee (20) were able to evaluate the polydispersity in scattering power numerically because they measured on proteins which are monodisperse with respect to size. In our case, however, this is impossible because also polydispersity in size does occur.

The value of M can also be related to the size of the particle: $M = \mathcal{N}_{AV}V\delta = \delta\mathcal{N}_{AV} \times (4/3)\pi a_M^3$. The radius a_M can be calculated if the density is known. The values of a_M are also given in Table II. The density figure used was 1.776 g cm^{-3}, as measured in cyclohexane dispersions.

If the mean value of the refractive index $\bar{n}_p$ is known we are able to interpret the variation in angular dependence using Eq. [17]. According to the Guinier approximation,

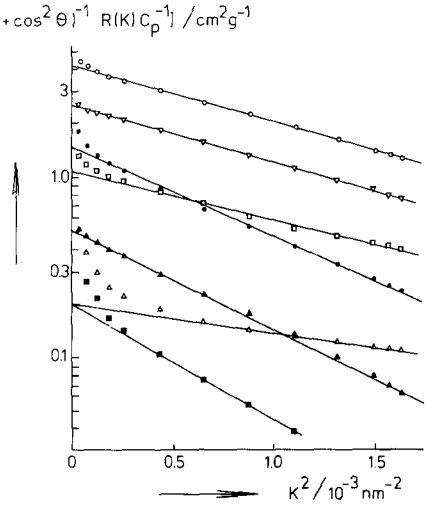

FIG. 4. Guinier plots for the light-scattering experiments from silica dispersions in various mixtures of cyclohexane and *t*-decahydronaphthalene. The mole-fraction of cyclohexane is ○, 0.00; ▽, 0.23; □, 0.46; △, 0.66; ■, 0.85; ▲, 0.91; ●, 1.00. The scattered intensity was measured with unpolarized incident light of λ_0 = 436 nm.

which is valid in the whole experimentally accessible K^2-region, the radius of gyration is found from the angular dependence,

$$\ln R(K) = -R_g^2K^2/3, \quad [32]$$

where R_g is given by Eq. [16], with $Q = (\bar{n}_p - n_0)V$.

A plot of R_g^2, determined from the Guinier plot [32], versus $(\bar{n}_p - n_0)^{-1}$, should yield a linear dependence as long as the third term is negligible. For very small contrast, i.e. $(\bar{n}_p - n_0)^{-1}$ very large, one can expect deviations from linearity. The radius of gyration of the equivalent homogeneous particle R_{g0} is found by interpolation to $(\bar{n}_p - n_0)^{-1} = 0$: the details of nonhomogeneity fluctuations do not contribute anymore when contrast tends to infinity.

In Fig. 6, R_g^2 is plotted vs $(\bar{n}_p - n_0)^{-1}$. The plot is approximately linear so we write,

$$R_g^2 \simeq R_{g0}^2 + E(\bar{n}_p - n_0)^{-1}. \quad [33]$$

From interpolation at $(n_p - n_0)^{-1} = 0$, R_{g0} is found which is expressed as $a_{R_g} \equiv [5R_{g0}^2/$

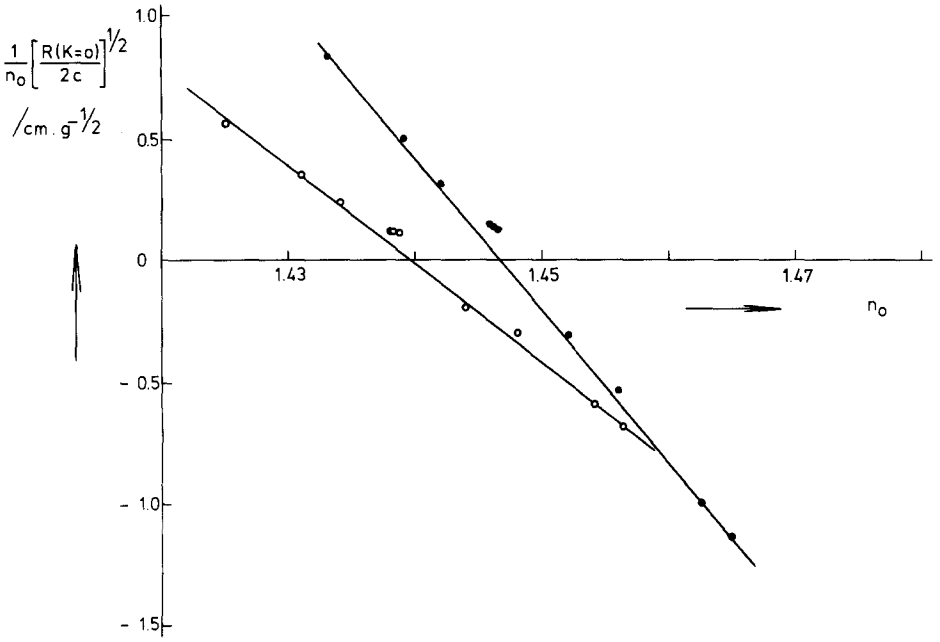

FIG. 5. The square root of the $K \rightarrow 0$ extrapolated scattered intensity is plotted versus the refractive index of the medium. The initial dispersion in cyclohexane is diluted with *t*-decaline. ○, λ_0 = 546 nm; ●, λ_0 = 436 nm.

3]$^{1/2}$, i.e., the radius of the equivalent sphere, in Table II.

The mean refractive index of the coated particle appears to be well within the range of values reported for amorphous silica's containing water (21). The low value of $\bar{n}_p$ cannot be explained by the presence of the layer of stearyl chains which is relatively thin.

The size calculated from R_{g0} (at infinite contrast) agrees well with the size determined from M, but is somewhat larger than the hydrodynamic size. The finite slope in Fig. 6 indicates that the particles are optically inhomogeneous. Its positive sign indicates a larger refractive index at the periphery than at the center.

Dilution from t-Decaline

Because contrast variation should be independent of the direction in which the dilution is started, dispersions in *t*-decaline were prepared and diluted with cyclohexane (see Fig. 7). Results of dilution in the opposite direction, taken from Fig. 5, are shown as dashed lines. It will be apparent that the plots do not fit properly but show systematic deviations. Because it was surmised that this effect could be related to preferent adsorption of one of the solvent components it was decided to study it more carefully.

VI. PREFERENT ADSORPTION OF A SOLVENT COMPONENT

Whereas the light-scattering measurements in the previous sections were per-

TABLE II

Parameters of SiO_2 Particles Determined with Contrast Variation

λ_0 (nm)	$(\mathcal{K}'M)^{1/2}$ (cm g$^{-1/2}$)	M (10^9 g mole^{-1})	a_M (nm)	$\bar{n}_p$	a_{R_g} (nm)	Slope E (Eq. [33]) (nm^2)
546	39	1.4	67	1.440	67.0	9
436	62	1.4	67	1.447	67.7	9

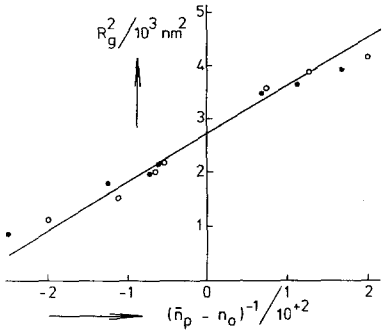

FIG. 6. The square of the optical radius of gyration is a linear function of the reciprocal of the contrast. ○, λ_0 = 546 nm; ●, λ_0 = 436 nm.

formed with a dilution series, it was decided to measure separate samples prepared in the appropriate solvent mixtures as well. Results for λ_0 = 546 nm are given in Fig. 8. It will be clear that the data points of the mixtures are below the (dashed) straight line connecting the data points of the pure solvents. This was also found with the dilution experiments (see Fig. 7), but the points in Fig. 8 are connected by a smooth curve and show a larger deviation. The dashed line intersects the n_0-axis at $n_0 = 1.441_7$ at λ_0 = 546 nm (and $n_0 = 1.448_6$ at λ_0 = 436 nm) which is nearly the same value as in Figs. 5 and 7. The slope of the dashed line gives $M = 1.1 \times 10^9$ g mole^{-1} ($M = 0.9 \times 10^9$ g mole^{-1} for λ_0 = 436 nm), which is somewhat smaller than the value found from Fig. 5. The curve intersects at $n_0 = 1.437_7$ (λ = 546 nm) and at $n_0 = 1.443_8$ (λ = 436 nm). The difference points to a positive adsorption of cyclohexane from the solvent mixture. Because the dashed and curved lines in Fig. 8 represent Q and Q_t, respectively, their difference, Q_σ, can be calculated and expressed in a measure of the adsorption Γ_1 of cyclohexane (called component 1), using Eq. [23].

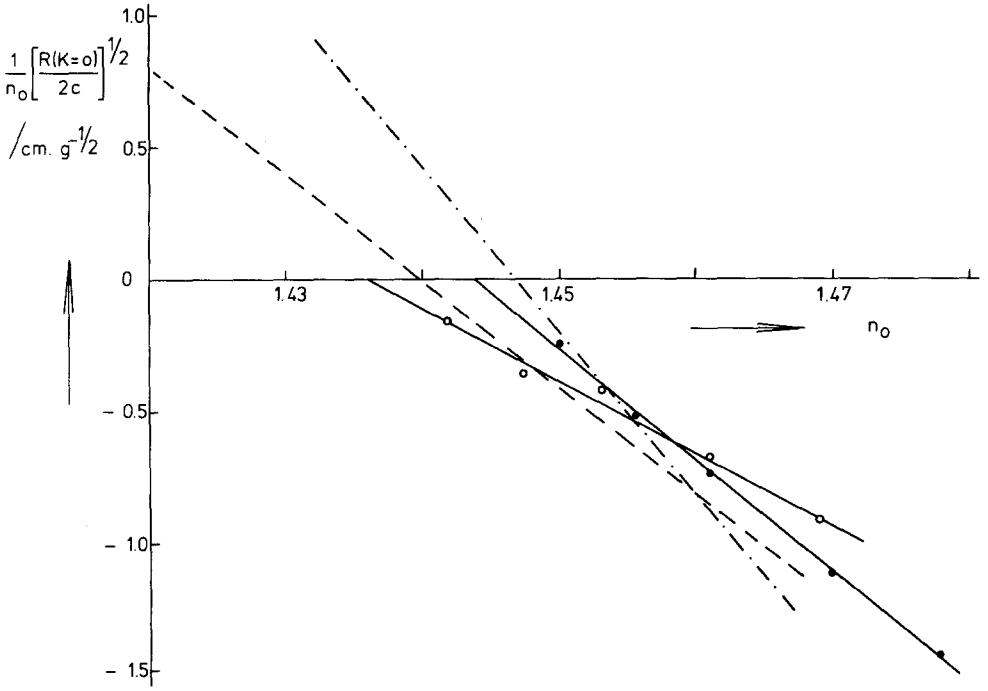

FIG. 7. The square root of the $K \to 0$ extrapolated scattered intensity is plotted versus the refractive index of the medium. ○, λ_0 = 546 nm; ●, λ_0 = 436 nm. The initial dispersion in *t*-decaline was diluted with cyclohexane. The dashed line represents the results from Fig. 5 (——), λ_0 = 546 nm; (–·–·–), λ_0 = 436 nm.

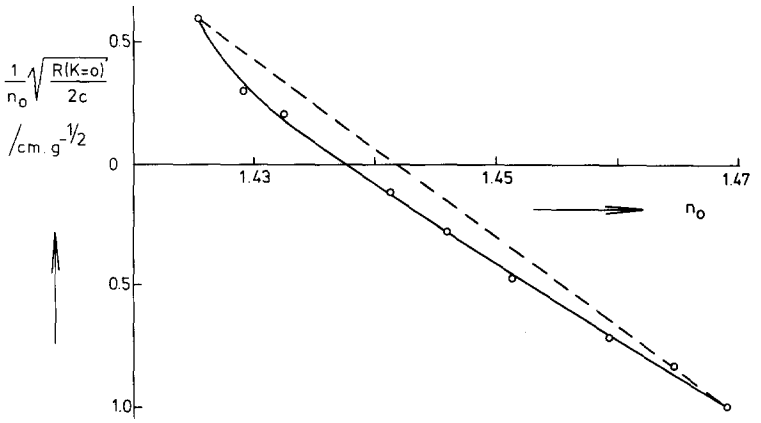

FIG. 8. The square root of the $K \to 0$ extrapolated scattered intensity is plotted versus the refractive index of the medium for $\lambda_0 = 546$ nm. The dispersions were prepared by suspending the dry silica in the appropriate solvent mixtures.

Results are shown in Table III. The refractive index increments $dn_0/d\psi_1$ were obtained with the help of the Lorentz–Lorenz equation, where ψ_1 is the mole fraction of cyclohexane. We used $M = 1.0 \times 10^9$ g mole^{-1}.

The quantities x_1 and y_1 in Table III give the number of moles of cyclohexane extracted from the mixture expressed per particle and per stearylalcohol chain, respectively. x_1 was calculated according to Strazielle (14) from Γ_1 with the equation $\Gamma_1 = x_1\bar{V}_1/M$, where $\bar{V}_1$ is the partial molar volume of component 1 (cyclohexane). We used for $\bar{V}_1$ the molar volume (=108.5 cm^3 mole^{-1}). The number of stearylalcohol chains was assessed from the carbon content of the particles and found to be ~2.8 $\times 10^5$ molecules per particle.

TABLE III

Adsorption of Cyclohexane by SiO_2 Particles from a Cyclohexane–*t*-Decaline Mixture[a]

ψ_1	$dn_0/d\psi_1$	Γ_1 (10^{-2} cm^3 g^{-1})	x_1 (10^5)	y_1
0.941	−0.063	4.2	3.9	1.4
0.885	−0.060	3.5	3.2	1.1
0.724	−0.052	3.3	3.0	1.1
0.627	−0.045	4.8	4.4	1.6
0.498	−0.040	4.6	4.2	1.5
0.293	−0.037	2.8	2.6	0.9
0.137	−0.033	0.1	0.1	0.03

[a] $\lambda_0 = 546$ nm. $c_p = 3.0$ g dm^{-3}.

The adsorption thus determined can be used to reinterpret the plot of R_g^2 versus reciprocal contrast. Neglecting the last term in Eq. [25], as done previously in Section V, one may write

$$R_g^2 = R_{g0}^2 + E'(\bar{n}_p + \Delta\bar{n}_p - n_0)^{-1}, \quad [34]$$

where $E' = E + Q_\sigma(R_{g\sigma}^2 + r_S^2 - R_{g0}^2)/V$. A plot of R_g^2 versus $(\bar{n}_p + \Delta\bar{n}_p - n_0)^{-1}$, analogous to Fig. 6, yielded $R_{g0}^2 = 2.37 \times 10^3$ nm^2 ($a_{R_g} = 62.9$ nm) and $E' = 11$ nm^2. From E' a value of E (see Eq. [33]) can be calculated by making some assumptions on the adsorbed liquid layer. If we assume that the optical center of the adsorbed layer coincides with the optical center of the equivalent homogeneous particle, ($r_S^2 = 0$), and that the adsorbed layer is thin compared with the particle size, ($R_{g\sigma}^2 \simeq a_{R_g}^2$), then E is found with [25] and [27] according to,

$$R_g^2 - \Delta\bar{n}_p(a_{R_g}^2 - R_{g0}^2)(\bar{n}_p + \Delta\bar{n}_p - n_0)^{-1} - R_{g0}^2 = E(\bar{n}_p + \Delta\bar{n}_p - n_0)^{-1}. \quad [35]$$

In Fig. 9 the left-hand side of this equation, containing only experimentally accessible parameters, is plotted against $(\bar{n}_p + \Delta\bar{n}_p - n_0)^{-1}$. Again a reasonable linear dependence is found with $E = 16$ nm^2.

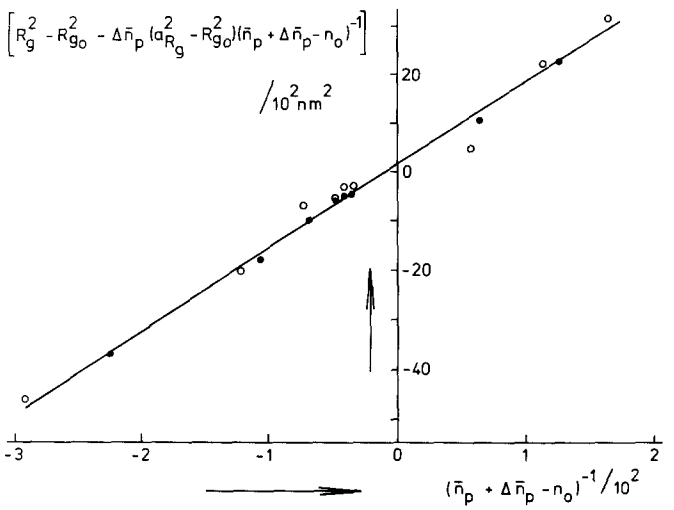

FIG. 9. Angular dependence corrected for preferential adsorption as a function of the reciprocal contrast. ○, λ_0 = 546 nm; ●, λ_0 = 436 nm. Further explanation is given in the text.

VII. DISCUSSION

The light-scattering method appears to be a powerful tool in characterizing these silica dispersions optically. The method is quite analogous to SAXS and SANS experiments which has been conducted by Stuhrmann and many others (1–4). In addition to the molar mass and the radius of gyration, one also gets information about the optical density (mean refractive index) and about the spatial distribution of optical density fluctuations. The low value of $\bar{n}_p$ which was found for the silica particles indicates a loose structure of the silica. Although the presence of an organic coating layer will probably decrease $\bar{n}_p$, the experimental values cannot be completely explained in this way, because the adsorbed layer is thin compared to the particle size. The low value of the density (δ = 1.776 g cm^{-3}) corroborates the conclusion that the structure deviates significantly from low-density crystalline silicas like β-tridymite or β-crystobatite: $n \sim 1.47$–1.48, $\delta \sim 2.3$ g cm^{-3} (21). In a further publication (17) where we shall report the results of different particle sizes and also include other experimental techniques, we shall go into more detail on this subject.

The molar mass which was found in the dilution experiment (see Table I) is somewhat higher than the value, calculated from the dashed line in Fig. 8. Probably the latter value is better, because the dashed line in Fig. 8 represents the scattering at $K = 0$ as it would be if the silica particle does not show preferential adsorption. One should be careful with this interpretation, however, because this is only valid when the scattering entity is physically equal in pure cyclohexane and in pure *t*-decaline.

For the dilution experiment (Table I) we found that the size a_{R_g}, calculated from R_{g0} at infinite contrast, is somewhat larger than the hydrodynamic radius a_D. The radius a_{R_g} agrees well with a_M, but probably both radii are somewhat too large. In our experiment with the separately prepared dispersions a_{R_g} compares very well with a_D and also reasonably with a_M (=61 nm).

Both in Figs. 6 and 9 a positive linear dependence is observed. This indicates that μ^2 and $(\mu + Q_\sigma r_S)^2$ are small. Apparently the optical centers *A*, *B*, *C*, and *S* practically coincide ($r_B = r_C = r_S = 0$). Alternatively one may say that the particle and adsorbed layer exhibit spherical symmetry in overall size and optical density fluctuations as well

TABLE IV

n_i Values Calculated from Experimental E Data[a]

	$n(\rho_i = 0)$	$n(\rho_i = a)$	$\bar{n}_p$
Dilution experiment			
$E = 9$ nm^2	1.406	1.451	1.440
Separately prepared dispersion			
$E = 11$ nm^2	1.400	1.456	1.442
$E = 16$ nm^2	1.382	1.462	1.442

[a] $\lambda_0 = 546$ nm. $a = 63$ nm.

(as far as the K^2 term is concerned). The sign and value of slope E yields an indication about the spatial distribution and magnitude of n_p fluctuations. $E \to Q_\beta(R^2_{g\beta} - R^2_{g\gamma})/V$ is positive means that $R_{g\beta} > R_{g\gamma}$, because $Q_\beta > 0$. In other words the refractive index of the periphery of the particle is larger than that of the core. We will now focus our attention on the numerical evaluation and discussion of E.

The spherical symmetry implies that E can be expressed as a function of the radial distance (ρ) from the optical center of gravity of the equivalent homogeneous particle. Recalling Eqs. [18] and [10] we can write for E, replacing the summation by an integration,

$$E = V^{-1} \int (n_i - \bar{n}_p)\rho_i^2 d^3\rho_i \qquad [34]$$

where $(n_i - \bar{n}_p)$ represents the local deviation of the refractive index at position ρ_i from the mean value $\bar{n}_p$. Because $Q_\beta + Q_\gamma = 0$ we also have $\int (n_i - \bar{n}_p)d^3\rho_i = 0$. It seemed reasonable first to try to explain the occurrence of refractive index fluctuations with the presence of the organic coating layer. We assumed the silica particle to be optically homogeneous coated with alkane chains with a different refractive index. Taking the thickness of the alkane layer 2 nm, we calculated for $E = 9$ nm^2 with $a = 63$ nm, a refractive index of the silica $n_{silica} = 1.434$ and $n_{alkane} = 1.500$, $\lambda_0 = 546$ nm. We think that the value of n_{alkane} is not very realistic. Therefore we must conclude that, although the coating layer might contribute to the optical inhomogeneity of the particle, it does not yield a satisfactory explanation of the measured E-data. The silica core itself must also be inhomogeneous to some extent at least.

If we assume another model for n_i as a function of ρ_i, for instance: $n_i(\rho_i) = \alpha\rho_i + n(\rho_i = 0)$ where $n(\rho_i = 0)$ is the refractive index at the center A of the particle and α is a coefficient describing the linear change of n_i with increasing distance, then one can derive $n_i(\rho_i) = \bar{n}_p + (5E/a^2)[(4\rho_i/a) - 3]$ with $0 \leq \rho_i \leq a$, and a being the radius of the particle.

We calculated $n_i(\rho_i)$ for both the dilution experiment and the experiment with separately prepared dispersions. For the latter experiment the calculation was done with $E = 11$ nm^2 (no adsorption correction) and $E = 16$ nm^2 (with adsorption correction). The results are shown in Table IV. We used $a = 63$ nm.

This calculation served as an example and aimed to be an illustration rather than being an attempt to provide the most realistic $n_i(\rho_i)$. It will be clear from Table IV, however, that the measured E-values, and thus the change of the radius of gyration with varying contrast, point to the occurrence of drastic variations of the refractive index within the particle. This in turn seems to indicate that the structure of the silica particle also shows large variations, the core being very loose and the outer region relatively compact.

The dilution experiment and the experiment with separately prepared dispersions do not give completely consistent results. This can be seen comparing Figs. 5, 7, and 8. Dilution of a dispersion with a second solvent yields a linear dependence in a plot of the square root of the intensity versus the refractive index of the medium. If the dispersions are prepared by adding the silica to the appropriate solvent mixtures a smoothly curved line is obtained. The discrepancy may be caused by the fact that the particle

concentration decreases upon dilution in the first experiment, whereas the concentration is approximately equal in the second. It was estimated, however, that deviation due to a nonneglectable second virial coefficient contribution is not likely to occur in the measured concentration region ($c \leq 3 \times 10^{-3}$ g cm^{-3}) unless the second virial coefficient is unexpected large. We calculated for a positive "hard-sphere" second virial coefficient that $[R_0/2c]^{1/2}/n_0$ decreases $\sim 1\%$ at $c = 3 \times 10^{-3}$ g cm^{-3}. This can be neglected regarding the experimental uncertainty. Another possible explanation might be a slowly equilibrating adsorption. The adsorption layer, which has been formed in the pure solvent, does change only very slowly upon addition of the second solvent. The result would be that the scattering unit (particle + adsorption layer) remains initially physically constant, thus producing a linear change of $(R_0/2c)^{1/2}/n_0$ with n_0. In the experiment all dispersions, however, were measured within a period of 8 hr. It seems likely that this time is long enough to ensure equilibrium, if adsorption takes place only at alkane chains on the particle surface. The effect of adsorption can be understood qualitatively. From Table III it can be seen that there is a preferential adsorption of $\sim$0.9–1.6 cyclohexane molecules at each alkane chain. Cyclohexane and *t*-decaline are both good solvents, but we expect cyclohexane to adsorb preferentially at the layer of alkane chains, because of a slightly better solvency in alkane chains (22) and possibly also due to the smaller size of the molecule. From the geometric surface of the particle (radius = 63 nm) we calculated a surface area of 0.18 nm^2 for each alkane chain. This value is very low, comparing the surface area in closely packed monolayers of soap molecules being 0.21 nm^2 (23). Consequently the geometric surface is a too low estimate of the real particle surface, but anyhow there is strong evidence that the surface layer of chains is rather dense. This in turn might cause some sterical hindering upon adsorption for the relatively large *t*-decaline molecules.

Quantitatively, the adsorption is quite large. Strazielle (14) reported that for polymers in binary solvents the adsorption is seldom higher than 0.5 molecule/monomer and if the second solvent is no longer a precipitant the adsorption does not exceed 0.18 molecule/monomer. Maybe we should think on adsorption of solvent molecules not only at the alkane molecules but also at the porous (17) silica surface itself. Considering the problems connected with the quantitative interpretation of the preferential adsorption phenomenon, we suggest for further similar investigations to use preferably (also) different pure solvents rather than solvent mixtures. If for a certain colloidal system a series of solvents can be found, which yield identical stable dispersions, then the light-scattering contrast variation method promises to be an interesting technique for particle characterization.

ACKNOWLEDGMENTS

Mr. H. Mos is gratefully thanked for making the dynamic light-scattering experiments and also Mr. J. Pieters for performing the electron microscope experiments. We wish to thank Mr. E. Nieuwenhuis for his helpful discussions and interest in our study. The authors are also indebted to Mr. W. A. den Hartog for the illustrations and to Miss H. Miltenburg for typing the manuscript.

REFERENCES

1. Kirste, R. G., and Stuhrmann, H. B., *Z. Phys. Chem., N.F.* **56,** 338 (1967).
2. Stuhrmann, H. B., *J. Appl. Crystallogr.* **7,** 173 (1974).
3. Cebula, D., Thomas, R. K., Harris, N. M., Tabony, I., and White, J. W., *J. Chem. Soc. Faraday Disc.* **65,** 76 (1978).
4. Taupin, C., Cotton, I. P., and Ober, R., *J. Appl. Crystallogr.* **11,** 613 (1978).
5. Vrij, A., and Overbeek, J. Th. G., *J. Colloid Sci.* **17,** 570 (1962).
6. Huisman, H. F., *Koninkl. Ned. Akad. Wetenschap. Proc. Ser.* **B67,** 367, 376, 388, 408 (1964).
7. Benoit, H., and Froelich, D., *in* "Light Scattering from Polymer Solutions" (M. D. Huglin, Ed.), p. 467. Academic Press, London, 1972.

8. Stuhrmann, H. B., *Z. Phys. Chem., N.F.* **72,** 177 (1970).
9. Vrij, A., Nieuwenhuis, E. A., Fijnaut, H. M., and Agterof, W. G. M., *J. Chem. Soc. Faraday Disc.* **65,** 101 (1978).
10. Nieuwenhuis, E. A., and Vrij, A., *J. Colloid Interface Sci.* **72,** 321 (1979).
11. Kerker, M., "The Scattering of Light and Other Electromagnetic Radiation." Academic Press, New York, 1969.
12. Debye, P., *J. Appl. Phys.* **15,** 338 (1944).
13. Cordier, P., *J. Chim. Phys.* **63,** 1158 (1966); **64,** 423 (1967).
14. Strazielle, C., *in* "Light Scattering from Polymer Solutions" (M. D. Huglin, Ed.), p. 633. Academic Press, London, 1972.
15. Stöber, W., Fink, A., and Bohn, E., *J. Colloid Interface Sci.* **26,** 62 (1968).
16. Iler, R. K., U. S. Patent 2,801,185.
17. Van Helden, A. K., Jansen, J. W. J., and Vrÿ, A., *J. Colloid Interface Sci.,* submitted for publication.
18. Johnson, B. L., and Smith, J., *in* "Light Scattering from Polymer Solutions" (M. D. Huglin, Ed.), p. 29. Academic Press, London, 1972.
19. Gomez-Ibanes, I. D., and Wang, T. C., *J. Phys. Chem.* **70,** 391 (1966).
20. Stuhrmann, H. B., and Duee, E. D., *J. Appl. Crystallogr.* **8,** 538 (1975).
21. Weast, R. C. (Ed.), "Handbook of Chemistry and Physics," 53rd ed., p. B-133. CRC Press, Cleveland, 1973.
22. Marcus, Y., "Introduction to Liquid State Chemistry." Wiley, London, 1977.
23. Rabinovitch, W., Robertson, R. F., and Mason, S. G., *Canad. J. Chem.* **38,** 1881 (1960).